



This is the accepted manuscript made available via CHORUS. The article has been published as:

Observation of an Inner-Shell Orbital Clock Transition in Neutral Ytterbium Atoms

Taiki Ishiyama, Koki Ono, Tetsushi Takano, Ayaki Sunaga, and Yoshiro Takahashi

Phys. Rev. Lett. **130**, 153402 — Published 14 April 2023

DOI: [10.1103/PhysRevLett.130.153402](https://doi.org/10.1103/PhysRevLett.130.153402)

Observation of an Inner-Shell Orbital Clock Transition in Neutral Ytterbium Atoms

Taiki Ishiyama, Koki Ono,* Tetsushi Takano, Ayaki Sunaga, and Yoshiro Takahashi
Department of Physics, Graduate School of Science, Kyoto University, Kyoto 606-8502, Japan
 (Dated: March 17, 2023)

We observe a weakly allowed optical transition of atomic ytterbium from the ground state to the metastable state $4f^{13}5d6s^2$ ($J = 2$) for all five bosonic and two fermionic isotopes with resolved Zeeman and hyperfine structures. This inner-shell orbital transition has been proposed as a new frequency standard as well as a quantum sensor for new physics. We find magic wavelengths through the measurement of the scalar and tensor polarizabilities and reveal that the measured trap lifetime in a three-dimensional optical lattice is 1.9(1) s, which is crucial for precision measurements. We also determine the g -factor by an interleaved measurement, consistent with our relativistic atomic calculation. This work opens the possibility of an optical lattice clock with improved stability and accuracy as well as novel approaches for physics beyond the Standard Model.

Recent development of optical atomic clocks using ions and neutral atoms has established a high fractional accuracy at the 10^{-18} level [1–3]. In addition to the contribution to metrology such as the redefinition of the second [4, 5] and geodesy [6, 7], a highly stable atomic clock enables various applications ranging from quantum simulations [8, 9] to fundamental physics [10] including gravitational wave detection [11], and others. The development of even more precise clocks benefits all of these applications.

Recently, the optical transition of atomic ytterbium (Yb) to its metastable state $4f^{13}5d6s^2$ ($J = 2$) with an energy of $23188.518 \text{ cm}^{-1}$ [12], has been proposed as a new frequency standard with high stability and accuracy [13, 14]. As shown in Fig. 1, the radiative lifetime of the $4f^{13}5d6s^2$ ($J = 2$) state is calculated to be much longer than that of the other metastable states, which potentially improves the quality factor of an optical lattice clock. In addition, the quadratic Zeeman shift as well as the black-body-radiation shift of the $^1S_0 \leftrightarrow 4f^{13}5d6s^2$ ($J = 2$) transition are calculated to be considerably small compared to those of the $^1S_0 \leftrightarrow ^3P_0$ and $^1S_0 \leftrightarrow ^3P_2$ transitions [14], suggesting that the inner-shell orbital clock transition has a potential to reduce systematic uncertainties. The dual clock operation [15] combined with the well-established $^1S_0 \leftrightarrow ^3P_0$ transition, or already observed $^1S_0 \leftrightarrow ^3P_2$ transition [16] of Yb atoms, possibly can further reduce systematic uncertainties in a clock comparison.

This metastable state of Yb also attracts considerable interest from the viewpoints of new physics searches [13, 14, 17]. The $^3P_0 \leftrightarrow 4f^{13}5d6s^2$ ($J = 2$) as well as $^3P_2 \leftrightarrow 4f^{13}5d6s^2$ ($J = 2$) [18] transitions show some of the highest sensitivities in neutral atoms to the variation of the fine-structure constant, providing also the possibilities of searching for ultralight scalar dark matter [19] and testing Einstein’s equivalence principle [10]. The metastable state has also high sensitivity to the violation of local Lorentz invariance in the electron-photon sector [17, 20], so far studied using single or two ions [21–24] and dysprosium atoms [25]. Furthermore, establishing a new clock

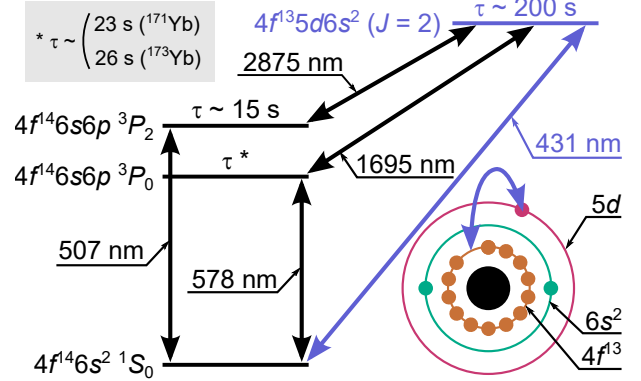


FIG. 1. Clock transitions in an Yb atom. The relevant transition wavelengths and lifetimes τ [14] are shown.

transition associated with the metastable state, in addition to the $^1S_0 \leftrightarrow ^3P_0$ and $^1S_0 \leftrightarrow ^3P_2$ transitions, provides a unique possibility to study a nonlinearity of the King plot using five bosonic isotopes of Yb in the search for a hypothetical particle mediating a force between electrons and neutrons beyond the Standard Model [26, 27]. Clearly, the first step towards these experiments is to experimentally observe the associated transition and characterizations such as the lifetime [13, 14, 18] and possible existence of a magic wavelength [14, 18].

In this Letter, we report the observation of the $^1S_0 \leftrightarrow 4f^{13}5d6s^2$ ($J = 2$) optical transition of Yb. The resonances for all five bosonic and two fermionic isotopes are clearly observed with resolved Zeeman and hyperfine structures. We find two magic wavelengths of 797.2(4) nm and 834.2(1) nm for the practical condition of $m_J = 0$ and the laser polarization perpendicular to a magnetic field, through the measurement of the polarizability. Here m_J is the projection of the total electronic angular momentum J along the quantization axis. In addition, our excitation and de-excitation sequence measurement of atoms in a three-dimensional optical lattice enables us to obtain the trap lifetime to be 1.9(1) s. Through an interleaved measurement with

different magnetic fields, we determine the g -factor to be $1.463(2)$, consistent with our relativistic many-body calculation. These findings are promising for the development of an optical lattice clock with improved stability and accuracy, and its various applications for searching for physics beyond the Standard Model.

Experimental setup. All spectroscopic measurements other than the lifetime measurement are done using ultracold Yb atoms evaporatively cooled in a crossed far-off resonance trap (FORT) [28]. The number of atoms is about $2 \times 10^4 \sim 1.3 \times 10^5$ and the temperature is about $0.3 \sim 1 \mu\text{K}$, depending on the isotope. We apply a linearly polarized excitation light beam at a wavelength of 431 nm. We measure the number of atoms remaining in the ground state after the irradiation of the excitation laser, and identify the optical resonance through the resonant atom loss. The angle of linear polarization, light intensity, and irradiation time are adjusted to optimize each spectroscopic measurement. We note that the lifetime measurement is done for atoms loaded into a three-dimensional (3D) optical lattice.

Zeeman and hyperfine spectra. Figure 2 summarizes the isotope shifts, Zeeman, and hyperfine spectra of the five bosonic isotopes (^{168}Yb , ^{170}Yb , ^{172}Yb , ^{174}Yb , and ^{176}Yb with nuclear spin $I = 0$) and the two fermionic isotopes (^{171}Yb and ^{173}Yb , with $I = 1/2$ and $5/2$, respectively). The upper panel of Fig. 2(a) shows the spectra of the five bosonic isotopes, and the lower panel shows m_J -resolved spectra of ^{174}Yb . The angle between the propagation (polarization) direction of the excitation light and the quantization axis, defined by a magnetic field, is $45^\circ(24^\circ)$. This configuration allows the excitation to all magnetic sublevels of the $4f^{13}5d6s^2$ ($J = 2$) state, according to the selection rule for a magnetic quadrupole (M2) transition. The typical full width at half maximum (FWHM) is about 30 kHz, limited by the Doppler broadening of about 20 kHz and the finite laser linewidth of about 10 kHz. Note that more than half of the atoms are lost at the peak, suggesting some atom loss mechanism in the $4f^{13}5d6s^2$ ($J = 2$) state, possibly caused by a shallow trapping potential and inelastic atom collisions.

Successful observation of the spectra of all bosonic isotopes enables us to determine the isotope shifts of the $1S_0 \leftrightarrow 4f^{13}5d6s^2$ ($J = 2$) transition [29]. The determined isotope shifts are summarized in Table I, where only the statistical errors are evaluated. Note that many systematic effects, such as the light shift and the quadratic Zeeman shift, are common among the isotopes within the accuracy of the present measurement. In order to evaluate a possible line shift due to s -wave collisions between trapped ultracold atoms, which would be the largest systematic effect among many, we perform interleaved measurements with two different numbers of atoms by adjusting the evaporative cooling process. For the five bosonic isotopes, the resonance shifts, corrected for the difference in the atomic temperature, are within the uncertainties of

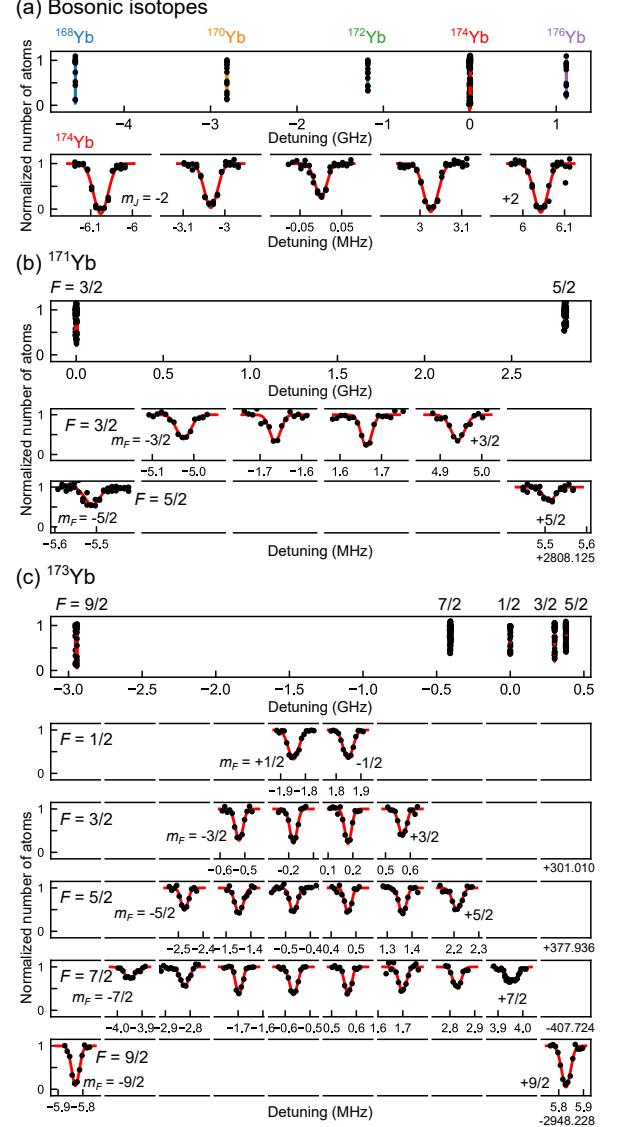


FIG. 2. Excitation spectra of all stable isotopes. (a) Five bosonic isotopes. The upper figure shows all spectra of the five isotopes for $m_J = 0$ state, except for ^{174}Yb , and the lower shows a magnified view around ^{174}Yb . The horizontal axis is the detuning from the resonance frequency of ^{174}Yb ($m_J = 0$). (b) Two fermionic isotopes, (b) ^{171}Yb ($I = 1/2$) and (c) ^{173}Yb ($I = 5/2$). The top figures show all spectra of all hyperfine states, and the lower show m_F -resolved spectra of each hyperfine state. The horizontal axis is the detuning from the average of $m_F = \pm 1/2$ in $F = 3/2$ for ^{171}Yb and $F = 1/2$ for ^{173}Yb . The solid curves are the fits with a Gaussian function. Note that not all the magnetic sublevels for $F = 5/2(9/2)$ state of ^{171}Yb (^{173}Yb) are shown.

about 5 kHz, and we find no evidence of atomic collision shifts at our measurement conditions.

In addition, we precisely determine the g -factor of the $4f^{13}5d6s^2$ ($J = 2$) state as $g_J = 1.463(2)$ with the uncertainty determined by the propagation of the fitting error and the uncertainty of the magnetic field calibra-

TABLE I. Measured isotope shifts $\nu^{A'A} := \nu^{A'} - \nu^A$ of the $4f^{14}6s^2\ ^1S_0 \leftrightarrow 4f^{13}5d6s^2\ (J=2)$ transition, where ν^A is the transition frequency of an Yb isotope with a mass number A . Statistical 1σ uncertainties are shown as $(\cdot)_{\text{stat}}$.

Isotope pair (A', A)	Isotope shift $\nu^{A'A}$ (MHz)
(168, 174)	$-4564.596\ (2)_{\text{stat}}$
(170, 174)	$-2810.666\ (2)_{\text{stat}}$
(172, 174)	$-1180.614\ (2)_{\text{stat}}$
(174, 176)	$-1115.766\ (6)_{\text{stat}}$

tion [30]. Our theoretical calculation of the g -factor using the DIRAC program [31, 32] gives $g_J = 1.465(2)$, which is consistent with the experiment [33].

Figures 2(b) and (c) shows the hyperfine (top panel) and Zeeman spectra (lower panels) of ^{171}Yb and ^{173}Yb , respectively. The observed Zeeman spectra for fermionic isotopes are well explained by the measured g_J . Here, we identify an excitation mechanism other than the M2 transition. A hyperfine interaction can cause the $4f^{13}5d6s^2\ (J=2)$ state to mix with other states such as 3P_1 and $4f^{13}5d6s^2\ (J=1)$ states, making the electric-dipole (E1) transition partially allowed, which is called a hyperfine-induced E1 transition [34]. The transition to the $F=3/2$ state of ^{171}Yb and those to the $F=3/2, 5/2$, and $7/2$ of ^{173}Yb are E1-allowed, and give resonance signals much stronger than other transitions that are allowed only by M2.

The data shown in Figs. 2(b) and (c) enable us to determine the hyperfine constants of ^{171}Yb and ^{173}Yb of the $4f^{13}5d6s^2\ (J=2)$ state, respectively [35]. We obtain the magnetic dipole constant $A_{\text{HFS}}(^{171}\text{Yb}) = 1123.3(3)$ MHz, and $A_{\text{HFS}}(^{173}\text{Yb}) = -309.46(4)$ MHz, and the electric quadrupole constant $B_{\text{HFS}}(^{173}\text{Yb}) = -1700.6(9)$ MHz, with the uncertainties due to the fitting error. Note that the presumably much smaller systematic effects such as the collision shift are not evaluated at present. The careful evaluation of the systematic effects and precise determination of the hyperfine constants will be an important future work. It is also noted that introducing a magnetic octupole constant C_{HFS} for ^{173}Yb does not improve the fitting.

Differential polarizability. We perform a measurement of the wavelength-dependent polarizability of the $4f^{13}5d6s^2\ (J=2)$ state. This is very important in the search for a magic wavelength at which the polarizabilities of the ground and $4f^{13}5d6s^2\ (J=2)$ states coincide, and thus the line shift due to the trapping light is largely suppressed, enabling ultra-narrow-linewidth spectroscopy and accurate clock operation [36].

In the case of linear polarization, the total polarizabil-

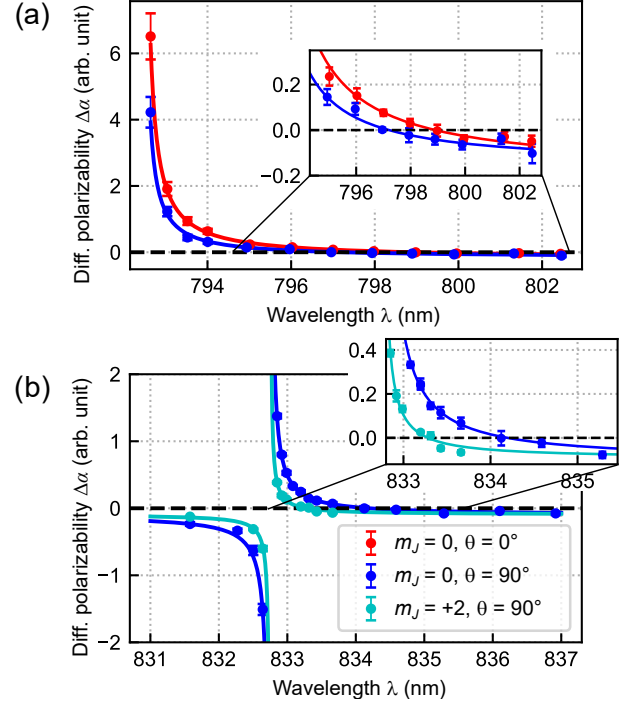


FIG. 3. Differential polarizability measurement between 1S_0 and $4f^{13}5d6s^2\ (J=2)$ states. Measurements around the transitions: (a) $4f^{13}5d6s^2\ (J=2) \leftrightarrow 4f^{13}6s^26p_{3/2}\ (J=3)$ at 792.5 nm, and (b) $4f^{13}5d6s^2\ (J=2) \leftrightarrow 4f^{13}6s^26p_{3/2}\ (J=2)$ at 833.7 nm. The differential polarizability, shown on the vertical axis as arbitrary units, is obtained from the linear fit to the measured differential light shifts $\Delta\nu$ as a function of the Ti:sapphire laser intensity. The error bars on the vertical axis are obtained from the error propagation of the standard error of $\Delta\nu$ and the uncertainty of the Ti:sapphire laser intensity. The solid curves are fits to the data.

ity α of the state $|J, m_J\rangle$ is

$$\alpha = \alpha^S + \frac{3\cos^2\theta - 1}{2} \frac{3m_J^2 - J(J+1)}{J(2J-1)} \alpha^T, \quad (1)$$

where the superscripts S and T denote scalar and tensor, respectively, and θ is the polarization angle with respect to the quantization axis [37]. Using this formula, the differential polarizability $\Delta\alpha$ between the ground state with $J=0$ and the $4f^{13}5d6s^2\ (J=2)$ state is given in a straightforward manner.

In this work, we search for a magic wavelength within the tunable range of a titanium(Ti):sapphire laser which can provide enough power for optical lattices [38]. In particular, in this wavelength range, there are two E1-allowed optical transitions of $4f^{13}5d6s^2\ (J=2) \leftrightarrow 4f^{13}6s^26p_{3/2}\ (J=3)$ at a wavelength of 792.5 nm and $4f^{13}5d6s^2\ (J=2) \leftrightarrow 4f^{13}6s^26p_{3/2}\ (J=2)$ at 832.7 nm [12], which will resonantly change the polarizability. In fact, according to our calculation for the excited state and Ref. [39] for the ground state, the magic

wavelengths are expected to be around 795.5 nm and 833.7 nm for $m_J = 0$ and $\theta = 90^\circ$ [40].

As shown in Fig. 3(a) and (b), we observe the resonant changes of the polarizability in the vicinity of the transition wavelengths of 792.5 nm and 832.7 nm. The solid curves are the fits to the data using the following equation: $\Delta\alpha(\omega) = a/(\omega_0^2 - \omega^2) + b$, where a and b are fitting parameters, ω is the angular frequency of a Ti:sapphire laser, and ω_0 is the resonance angular frequency of the $4f^{13}5d6s^2 (J=2) \leftrightarrow 4f^{13}6s^26p_{3/2} (J=3)$ or $4f^{13}5d6s^2 (J=2) \leftrightarrow 4f^{13}6s^26p_{3/2} (J=2)$ transition, given in Ref. [12]. Note that this model assumes that only one resonant transition with ω_0 dominantly contributes to the wavelength dependence, while the effects of other off-resonant transitions contribute as wavelength-independent offset constant b . From the fitting, we can determine the magic wavelengths λ_{magic} as follows:

$$\lambda_{\text{magic}} = \begin{cases} 798.9(4) \text{ nm} & (m_J = 0, \theta = 0^\circ), \\ 797.2(4) \text{ nm} \\ 834.2(1) \text{ nm} \\ 833.28(4) \text{ nm} \end{cases} \begin{cases} (m_J = 0, \theta = 90^\circ), \\ (m_J = 2, \theta = 90^\circ). \end{cases} \quad (2)$$

Since two measurements with different θ or m_J at each wavelength are performed, we can determine the differential scalar polarizability $\Delta\alpha^S$ and the tensor polarizability α^T from Eq. (1). Possible trap geometries to minimize the uncertainty of the tensor light shift on the performance of clock operation using the 797.2-nm optical lattice are discussed in Supplemental Material [41]. It should be noted that the differential higher-order light shift due to M1 and E2 multipolar polarizabilities and E1 hyperpolarizability [42] should exist even at an E1 magic wavelength, where the differential light shift due to E1 polarizability vanishes [36]. The investigation of the operational magic condition for wavelength and intensity, where the overall light shift is insensitive to the lattice-intensity variation [43], will be an important future work for clock operation.

Lifetime. The lifetime of the excited state of a clock transition is important because it is directly related to the quality factor of the clock transition. In this measurement, we use spin-polarized ^{173}Yb atoms in the $|F=5/2, m_F=5/2\rangle$ state loaded into a 3D optical lattice to minimize the possible atom loss due to inelastic interatomic collisions. The 3D optical lattice consists of a 2D optical lattice at the wavelength $\lambda_1 = 759.4$ nm and a 1D optical lattice at the wavelength $\lambda_2 = 797.2$ nm, superimposed on the excitation light [44]. Figure. 4 shows the number of excited atoms as a function of the holding time in the optical lattice. The lattice depths are $28E_R$ for the 2D optical lattice at λ_1 , and $25E_R$ for the 1D optical lattice at λ_2 . Here $E_R = \hbar^2/(2m\lambda_2^2) = \hbar \times 1.8$ kHz represents the recoil energy at the wavelength λ_2 , where \hbar is the Planck constant, and m is the mass of an Yb atom.

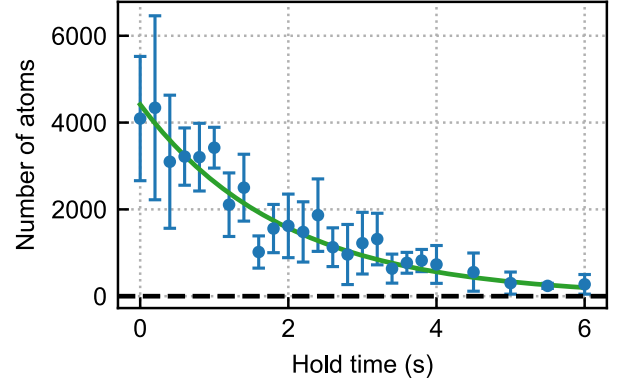


FIG. 4. Lifetime measurement of atoms in $4f^{13}5d6s^2 (J=2)$ state. The horizontal axis shows the time to hold the excited atoms in the optical lattice, and the vertical axis shows the number of atoms in the excited state after the hold time. The measurements are repeated four times, and the mean and standard deviation are plotted.

From the fit to the data with a single exponential function, the trap lifetime of the excited atoms is obtained as 1.9(1) s. As a reference, we also investigate the trap loss of atoms in the ground state 1S_0 in the same experimental setup, and find the trap lifetime to be 2.8(2) s, which would be limited by some mechanism such as collisions with background gases. Assuming that the same mechanism also limits the trap lifetime of the $4f^{13}5d6s^2 (J=2)$ state, we infer the intrinsic state lifetime of the excited state to be 5.9(1.3) s. This is compared with the theoretical calculations in Refs. [14], [13], and [18], which predict a lifetime of about 200 s, 60 s, and 190 s, respectively. Our preliminary estimation shows that the rate of the photon scattering γ_{sc} due to the lattice laser beam of near resonant 797.2-nm light at $25E_R$ is $\gamma_{\text{sc}} = 0.15 \text{ s}^{-1}$, which seemingly explains the measured result. Further systematic measurements with various experimental conditions will clarify the intrinsic lifetime of this state.

Summary. We report the observation of the $^1S_0 \leftrightarrow 4f^{13}5d6s^2 (J=2)$ optical transition of all seven Yb isotopes with resolved Zeeman and hyperfine structures. Two magic wavelengths of 797.2(4) nm and 834.2(4) nm for practical conditions are found and the measured lifetime is 1.9(1) s, promising for applications for precision measurements. We also determine the g -factor to be 1.463(2), and compare the result with our relativistic many-body calculation with good agreement. A 3D optical lattice experiment with many ultracold atoms with isotope mixtures for the observed $4f^{13}5d6s^2 (J=2)$ state is promising to test the violation of local Lorentz invariance of electron-photon sector and Einstein's weak equivalence principle.

This work was supported by the Grant-in-Aid for Scientific Research of JSPS (Nos. JP17H06138, JP18H05405, JP18H05228, JP20K14383, JP21H01014,

JP22K20356), JST CREST (No. JP-MJCR1673), and MEXT Quantum Leap Flagship Program (MEXT Q-LEAP) Grant No. JPMXS0118069021, and , JST Moonshot R&D-MILLENNIA Program (Grant No. JP-MJMS2269). K.O. was supported by Graduate School of Science, Kyoto University under Ginpu Fund. A.S. acknowledges support from the JSPS KAKENHI Grant No. 21K14643. In this research work, A.S. used the computer resource offered under the category of General Projects by the Research Institute for Information Technology, Kyushu University.

* koukiono3@yagura.scphys.kyoto-u.ac.jp

- [1] C. W. Chou, D. B. Hume, J. C. J. Koelemeij, D. J. Wineland, and T. Rosenband, Frequency Comparison of Two High-Accuracy Al^+ Optical Clocks, *Phys. Rev. Lett.* **104**, 070802 (2010).
- [2] B. J. Bloom, T. L. Nicholson, J. R. Williams, S. L. Campbell, M. Bishof, X. Zhang, W. Zhang, S. L. Bromley, and J. Ye, An optical lattice clock with accuracy and stability at the 10^{-18} level, *Nature* **506**, 71 (2014).
- [3] I. Ushijima, M. Takamoto, M. Das, T. Ohkubo, and H. Katori, Cryogenic optical lattice clocks, *Nature Photonics* **9**, 185 (2015).
- [4] C. Grebing, A. Al-Masoudi, S. Dörscher, S. Häfner, V. Gerginov, S. Weyers, B. Lipphardt, F. Riehle, U. Sterr, and C. Lisdat, Realization of a timescale with an accurate optical lattice clock, *Optica* **3**, 563 (2016).
- [5] W. R. Milner, J. M. Robinson, C. J. Kennedy, T. Bothwell, D. Kedar, D. G. Matei, T. Legero, U. Sterr, F. Riehle, H. Leopardi, *et al.*, Demonstration of a Timescale Based on a Stable Optical Carrier, *Phys. Rev. Lett.* **123**, 173201 (2019).
- [6] T. Takano, M. Takamoto, I. Ushijima, N. Ohmae, T. Akatsuka, A. Yamaguchi, Y. Kuroishi, H. Munekane, B. Miyahara, and H. Katori, Geopotential measurements with synchronously linked optical lattice clocks, *Nature Photonics* **10**, 662 (2016).
- [7] C. Lisdat, G. Grosche, N. Quintin, C. Shi, S. M. F. Raupach, C. Grebing, D. Nicolodi, F. Stefani, A. Al-Masoudi, S. Dörscher, *et al.*, A clock network for geodesy and fundamental science, *Nature Communications* **7**, 12443 (2016).
- [8] S. Kato, K. Inaba, S. Sugawa, K. Shibata, R. Yamamoto, M. Yamashita, and Y. Takahashi, Laser spectroscopic probing of coexisting superfluid and insulating states of an atomic Bose–Hubbard system, *Nature Communications* **7**, 11341 (2016).
- [9] S. Kolkowitz, S. L. Bromley, T. Bothwell, M. L. Wall, G. E. Marti, A. P. Koller, X. Zhang, A. M. Rey, and J. Ye, Spin–orbit-coupled fermions in an optical lattice clock, *Nature* **542**, 66 (2017).
- [10] M. S. Safronova, D. Budker, D. DeMille, D. F. J. Kimball, A. Derevianko, and C. W. Clark, Search for new physics with atoms and molecules, *Rev. Mod. Phys.* **90**, 025008 (2018).
- [11] S. Kolkowitz, I. Pikovski, N. Langellier, M. D. Lukin, R. L. Walsworth, and J. Ye, Gravitational wave detection with optical lattice atomic clocks, *Phys. Rev. D* **94**, 124043 (2016).
- [12] A. Kramida, Y. Ralchenko, J. Reader, and NIST ASD Team, NIST Atomic Spectra Database (version 5.10) [Online], Available: <https://physics.nist.gov/asd> [2023, January 03]. National Institute of Standards and Technology, Gaithersburg, MD. (2022).
- [13] M. S. Safronova, S. G. Porsev, C. Sanner, and J. Ye, Two Clock Transitions in Neutral Yb for the Highest Sensitivity to Variations of the Fine-Structure Constant, *Phys. Rev. Lett.* **120**, 173001 (2018).
- [14] V. A. Dzuba, V. V. Flambaum, and S. Schiller, Testing physics beyond the standard model through additional clock transitions in neutral ytterbium, *Phys. Rev. A* **98**, 022501 (2018).
- [15] D. Akamatsu, T. Kobayashi, Y. Hisai, T. Tanabe, K. Hosaka, M. Yasuda, and F.-L. Hong, Dual-Mode Operation of an Optical Lattice Clock Using Strontium and Ytterbium Atoms, *IEEE Transactions on Ultrasonics, Ferroelectrics, and Frequency Control* **65**, 1069 (2018).
- [16] A. Yamaguchi, S. Uetake, S. Kato, H. Ito, and Y. Takahashi, High-resolution laser spectroscopy of a Bose–Einstein condensate using the ultranarrow magnetic quadrupole transition, *New Journal of Physics* **12**, 103001 (2010).
- [17] R. Shaniv, R. Ozeri, M. S. Safronova, S. G. Porsev, V. A. Dzuba, V. V. Flambaum, and H. Häfner, New Methods for Testing Lorentz Invariance with Atomic Systems, *Phys. Rev. Lett.* **120**, 103202 (2018).
- [18] Z.-M. Tang, Y.-m. Yu, B. K. Sahoo, C.-Z. Dong, Y. Yang, and Y. Zou, A New Clock Transition with the Highest Sensitivity to α Variation and Simultaneous Magic Trapping Conditions with Other Clock Transitions in Yb, *arXiv:2208.09200*.
- [19] A. Arvanitaki, J. Huang, and K. Van Tilburg, Searching for dilaton dark matter with atomic clocks, *Phys. Rev. D* **91**, 015015 (2015).
- [20] V. A. Kostelecký and C. D. Lane, Constraints on lorentz violation from clock-comparison experiments, *Phys. Rev. D* **60**, 116010 (1999).
- [21] T. Pruttivarasin, M. Ramm, S. G. Porsev, I. I. Tupitsyn, M. S. Safronova, M. A. Hohensee, and H. Häfner, Michelson–Morley analogue for electrons using trapped ions to test Lorentz symmetry, *Nature* **517**, 592 (2015).
- [22] E. Megidish, J. Broz, N. Greene, and H. Häfner, Improved Test of Local Lorentz Invariance from a Deterministic Preparation of Entangled States, *Phys. Rev. Lett.* **122**, 123605 (2019).
- [23] C. Sanner, N. Huntemann, R. Lange, C. Tamm, E. Peik, M. S. Safronova, and S. G. Porsev, Optical clock comparison for Lorentz symmetry testing, *Nature* **567**, 204 (2019).
- [24] L. S. Dreissen, C.-H. Yeh, H. A. Fürst, K. C. Grenseman, and T. E. Mehlstäubler, Improved bounds on Lorentz violation from composite pulse Ramsey spectroscopy in a trapped ion, *Nature Communications* **13**, 7314 (2022).
- [25] M. A. Hohensee, H. Müller, and R. B. Wiringa, Equivalence Principle and Bound Kinetic Energy, *Phys. Rev. Lett.* **111**, 151102 (2013).
- [26] J. C. Berengut, D. Budker, C. Delaunay, V. V. Flambaum, C. Fruguele, E. Fuchs, C. Grojean, R. Harnik, R. Ozeri, G. Perez, and Y. Soreq, Probing new long-range interactions by isotope shift spectroscopy, *Phys. Rev. Lett.* **120**, 091801 (2018).

- [27] K. Ono, Y. Saito, T. Ishiyama, T. Higomoto, T. Takano, Y. Takasu, Y. Yamamoto, M. Tanaka, and Y. Takahashi, Observation of Nonlinearity of Generalized King Plot in the Search for New Boson, *Phys. Rev. X* **12**, 021033 (2022).
- [28] See Sec. S1 in Supplemental Material [url] for the detail of the experimental system, which includes Refs. [27, 45–47].
- [29] See Sec. S2 in Supplemental Material [url] for the detail of the measurement procedure.
- [30] See Sec. S3 in Supplemental Material [url] for the detail of the measurement procedure, which includes Refs. [14, 48, 49].
- [31] T. Saue, R. Bast, A. S. P. Gomes, H. J. A. Jensen, L. Visscher, I. A. Aucar, R. Di Remigio, K. G. Dyall, E. Eliav, E. Fasshauer, *et al.*, The DIRAC code for relativistic molecular calculations, *J. Chem. Phys.* **152**, 204104 (2020).
- [32] DIRAC, a relativistic ab initio electronic structure program, Release DIRAC22 (2022), written by H. J. Aa. Jensen, R. Bast, A. S. P. Gomes, T. Saue and L. Visscher *et al.* (available at <http://dx.doi.org/10.5281/zenodo.6010450>, see also <http://www.diracprogram.org>), accessed Sep. 29, 2022.
- [33] See Sec. S7 in Supplemental Material [url] for the detail of the theoretical calculations, which includes Refs. [31, 32, 58–62].
- [34] M. M. Boyd, T. Zelevinsky, A. D. Ludlow, S. Blatt, T. Zanon-Willette, S. M. Foreman, and J. Ye, Nuclear spin effects in optical lattice clocks, *Phys. Rev. A* **76**, 022510 (2007).
- [35] See Sec. S4 in Supplemental Material [url] for the detail of the analysis, which includes Refs. [34, 50–53].
- [36] H. Katori, M. Takamoto, V. G. Pal’chikov, and V. D. Ovsiannikov, Ultrastable Optical Clock with Neutral Atoms in an Engineered Light Shift Trap, *Phys. Rev. Lett.* **91**, 173005 (2003).
- [37] F. Le Kien, P. Schneeweiss, and A. Rauschenbeutel, Dynamical polarizability of atoms in arbitrary light fields: general theory and application to cesium, *The European Physical Journal D* **67**, 92 (2013).
- [38] See Sec. S5B in Supplemental Material [url] for the detail of the measurement procedure, which includes Ref. [54].
- [39] Z.-M. Tang, Y.-M. Yu, J. Jiang, and C.-Z. Dong, Magic wavelengths for the transition in ytterbium atom, *Journal of Physics B: Atomic, Molecular and Optical Physics* **51**, 125002 (2018).
- [40] See Sec. S5A in Supplemental Material [url] for the detail of the theoretical calculations, which includes Refs. [37, 39].
- [41] See Sec. S5C in Supplemental Material [url] for the discussion, which includes Refs. [55–57].
- [42] S. G. Porsev, M. S. Safronova, U. I. Safronova, and M. G. Kozlov, Multipolar Polarizabilities and Hyperpolarizabilities in the Sr Optical Lattice Clock, *Phys. Rev. Lett.* **120**, 063204 (2018).
- [43] I. Ushijima, M. Takamoto, and H. Katori, Operational Magic Intensity for Sr Optical Lattice Clocks, *Phys. Rev. Lett.* **121**, 263202 (2018).
- [44] See Sec. S6 in Supplemental Material [url] for the detail of the measurement procedure.
- [45] S. Taie, Y. Takasu, S. Sugawa, R. Yamazaki, T. Tsujimoto, R. Murakami, and Y. Takahashi, Realization of a $SU(2) \times SU(6)$ System of Fermions in a Cold Atomic Gas, *Phys. Rev. Lett.* **105**, 190401 (2010).
- [46] X. Baillard, A. Gauguier, S. Bize, P. Lemonde, P. Laurent, A. Clairon, and P. Rosenbusch, Interference-filter-stabilized external-cavity diode lasers, *Optics Communications* **266**, 609 (2006).
- [47] R. W. P. Drever, J. L. Hall, F. V. Kowalski, J. Hough, G. M. Ford, A. J. Munley, and H. Ward, Laser phase and frequency stabilization using an optical resonator, *Applied Physics B* **31**, 97 (1983).
- [48] B. Budick and J. Snir, g_j values of excited states of the ytterbium atom, *Physics Letters A* **24**, 689 (1967).
- [49] M. Baumann and G. Wandel, g_j factors of the $6s6p\ ^3P_1$ and $6s6p\ ^1P_1$ states of ytterbium, *Physics Letters A* **28**, 200 (1968).
- [50] C. Schwartz, Theory of Hyperfine Structure, *Phys. Rev.* **97**, 380 (1955).
- [51] L. Olschewski, Messung der magnetischen kerndipolmomente an freien ^{43}Ca -, ^{87}Sr -, ^{135}Ba -, ^{137}Ba -, ^{171}Yb - und ^{173}Yb -Atomen mit optischem pumpen, *Zeitschrift für Physik* **249**, 205 (1972).
- [52] N. J. Stone, Table of nuclear magnetic dipole and electric quadrupole moments, *At. Data Nucl. Data Tables* **90**, 75 (2005).
- [53] S. G. Porsev, A. Derevianko, and E. N. Fortson, Possibility of an optical clock using the $6^1S_0 \rightarrow 6^3P_0^o$ transition in $^{171,173}\text{Yb}$ atoms held in an optical lattice, *Phys. Rev. A* **69**, 021403 (2004).
- [54] A. V. Taichenachev, V. I. Yudin, C. W. Oates, C. W. Hoyt, Z. W. Barber, and L. Hollberg, Magnetic Field-Induced Spectroscopy of Forbidden Optical Transitions with Application to Lattice-Based Optical Atomic Clocks, *Phys. Rev. Lett.* **96**, 083001 (2006).
- [55] T. Akatsuka, M. Takamoto, and H. Katori, Optical lattice clocks with non-interacting bosons and fermions, *Nature Physics* **4**, 954 (2008).
- [56] M. Takamoto, F.-L. Hong, R. Higashi, Y. Fujii, M. Imae, and H. Katori, Improved Frequency Measurement of a One-Dimensional Optical Lattice Clock with a Spin-Polarized Fermionic ^{87}Sr Isotope, *Journal of the Physical Society of Japan* **75**, 104302 (2006).
- [57] A. W. Young, W. J. Eckner, W. R. Milner, D. Kedar, M. A. Norcia, E. Oelker, N. Schine, J. Ye, and A. M. Kaufman, Half-minute-scale atomic coherence and high relative stability in a tweezer clock, *Nature* **588**, 408 (2020).
- [58] K. G. Dyall and A. S. Gomes, Revised relativistic basis sets for the 5d elements Hf-Hg, *Theoretical Chemistry Accounts* **125**, 97–100 (2010).
- [59] T. Fleig, J. Olsen, and L. Visscher, The generalized active space concept for the relativistic treatment of electron correlation. II. Large-scale configuration interaction implementation based on relativistic 2- and 4-spinors and its application, *J. Chem. Phys.* **119**, 2963 (2003).
- [60] S. Knecht, H. J. A. Jensen, and T. Fleig, Large-scale parallel configuration interaction. II. Two- and four-component double-group general active space implementation with application to BiH, *J. Chem. Phys.* **132**, 014108 (2010).
- [61] Stefan R. Knecht. Parallel Relativistic Multiconfiguration Methods: New Powerful Tools for Heavy-Element Electronic-Structure Studies. PhD thesis, Mathematisch-Naturwissenschaftliche Fakultät, Heinrich-Heine-Universität Düsseldorf, 2009. URL: <http://docserv.uni-duesseldorf.de/servlets/DocumentServlet?id=13226>.

- [62] M. Denis, M. S. Nørby, H. J. A. Jensen, A. S. P. Gomes, M. K. Nayak, S. Knecht, and T. Fleig, Theoretical study on ThF^+ , a prospective system in search of time-reversal violation, [New Journal of Physics](#) **17**, 043005 (2015).